Research on Hip Torque Control of Humanoid Unmanned Platform

Kaiyuan Wang(✉), Xuefeng Peng, Zhenkai Xiong, and Zongmiao Dai

9th Laboratory, 713th Research Institute of China Shipbuilding Industry Corporation, Zhengzhou 450000, Henan, China

Abstract. In order to make the humanoid unmanned platform show excellent control quality, it is necessary to design a high-performance joint drive system first. The humanoid unmanned platform has a large load, and the hydraulic drive mode has the highest power density ratio, so the hydraulic drive mode is chosen in this paper. Because of the needs of lightweight and compact structure, it is impossible to install torque sensors at the joints, so the calculation of joint torque control is the basic control strategy for the torque control of the hip joint. Firstly, the mathematical analysis of the hip four-link mechanism is carried out, and the relationship between the moment arm of the cylinder and the angle of the hip joint is calculated. Then the simulation is carried out in Maplesim, and the correctness of the calculated moment arm is preliminarily verified. Finally, the variable PID control is carried out by using the thrust of the cylinder and the torque of the hip joint obtained from the calculating moment arm as feedback, and the experimental verification is carried out on the prototype, and the results show the feasibility of the proposed method.

Keywords: Humanoid Unmanned Platform · Torque Control

1 Background

As a kind of nonlinear, multivariable and highly coupled complex mechanical device [1], humanoid unmanned platform has a very wide range of research fields. Among them, joint drive and control technology respectively provide power and control instructions for humanoid unmanned platform [2], which is undoubtedly an extremely important link in many research fields. The driving performance and control quality of the joint are the key factors affecting the final output of the humanoid unmanned platform [3]. Only on the basis of high-performance joint drive control system, it is meaningful to discuss the control technology [4]. In order to make the humanoid unmanned platform have good motion characteristics, the structure should be as simple and light as possible. In the joint drive system design, the common driving methods include motor drive, hydraulic drive and pneumatic drive. When driven by motor, in order to provide the large torque required for motion, a reducer is essential. This will make the joints become too heavy. Although pneumatic drive structure is simple, the power is low and it is difficult to control accurately. Compared with the former, the hydraulic drive power density ratio is high,

M. Wu et al. (Eds.): ICAUS 2021, LNEE 861, pp. 448–456, 2022.
https://doi.org/10.1007/978-981-16-9492-9_45

and the structure is relatively simple. To sum up, hydraulic drive is the optimal way of joint drive. Usually, the single joint torque control of the humanoid unmanned platform is based on the feedback of torque sensor [5]. However, the humanoid unmanned platform designed in this paper cannot install torque sensor due to the demands of lightweight and compact structure, so the torque control can only be obtained by calculating the feedback value of torque through the thrust and moment arm of the oil cylinder. The thrust of the cylinder can be obtained by a pressure sensor mounted on the cylinder, and the moment arm is time-varying and cannot be measured directly. Therefore, it is necessary to analyze the hip four-bar mechanism.

2 Calculation and Simulation

The hip four-bar mechanism of the humanoid unmanned platform is shown in Fig. 1. Since the moment arm of the hydraulic cylinder on the hip joint is constantly changing and cannot be measured directly, it is necessary to calculate the value of the moment arm to calculate the moment of the cylinder on the hip joint.

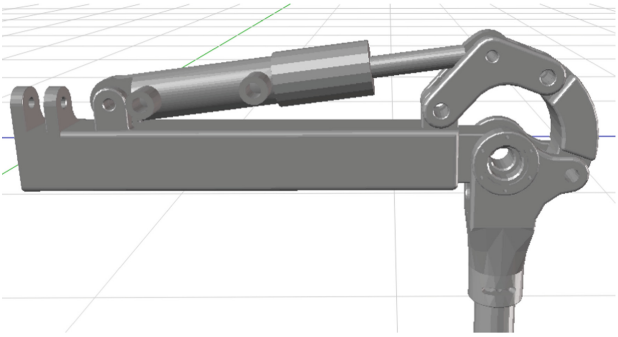

Fig. 1. 3D model of hip four-bar mechanism.

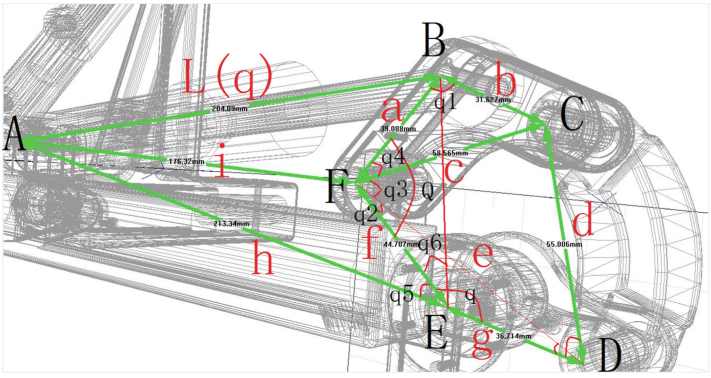

Fig. 2. Explosion diagram of the mechanism.

The relationship between the total length of the cylinder of the four-link mechanism L(t) and the hip joint angle q can be calculated according to Fig. 2. L(t) is the distance between point A and B which represents the total length of the cylinder and is a variable.

The distance between B and F is expressed by *a*, which is a fixed value; The distance between B and C is expressed by b, which is a fixed value; The distance between C and F is expressed by c, which is a fixed value; The distance between C and D is denoted by d, which is a variable; The distance between D and F is denoted by e, which is a variable; The distance between E and F is expressed by f, which is a constant value; The distance between D and E is expressed by g, which is a constant value; The distance between A and E is expressed by h, which is a constant value; The distance between A and F is denoted by i, which is a constant value.

Angle DEF, expressed by q, is a variable; Angle CBF is expressed by q1, which is a constant value; Angle DFE, expressed by q2, is a variable; Angle CFD, expressed by q3, is a variable; Angle BFC is expressed by q4, which is a constant value; Angle AEF, expressed by q5, is a constant value; Angle BEF, expressed by q6, is a variable; Angle BFE, denoted by Q, is a variable.

When the hip joint is in the initial position, q is 2.63rad, and the hip joint angle q (t) is obtained through the encoder. In the triangle DEF, e can be obtained through the law of cosine:

$$e = \sqrt{\left(f^2 + g^2 - 2 * f * g * \cos(2.63 - q(t))\right)} \tag{1}$$

In the triangle DEF and CDF, q2(t) and q3(t) can be obtained by the law of sine and cosine respectively. In triangle BCF, angle BFC is fixed, i.e. q4 = 0.5268rad, so angle BFE can be obtained. In the triangle BEF, the distance of B and E is n(t), and n(t) can be obtained by the law of cosine. In triangle BEF, q6(t) can be obtained by the law of sine. In the triangle AEF, the angle AEF is fixed, that is, q5 = 0.569 rad. In the triangle ABE, angle AEB is the sum of q5(t) and q6(t), L(t) can be obtained by the law of cosine:

$$L(t)=\sqrt{(h * h + n(t) * n(t) - 2 * h * n(t) * \cos(0.569 + q6(t)))} \tag{2}$$

The expansion of the oil cylinder L(t) is L(t) minus the initial length of the cylinder 0.20622 m, i.e.

$$L'(t)=\sqrt{(h * h + n(t) * n(t) - 2 * h * n(t) * \cos(0.569 + q6(t)))} - 0.20622 \tag{3}$$

In triangle ABF, angle BAF can be obtained by the law of cosine. In the triangle ABE, angle BAE is the sum of angle BAF and angle EAF, and angle EAF is a fixed value, that is 0.128 rad. Vertical line AB across point E is the moment arm lm (t) of the cylinder's thrust on the hip joint. The moment arm can be obtained by using the law of sine:

$$lm(t) = h * \sin(0.128 + \angle BAF) \tag{4}$$

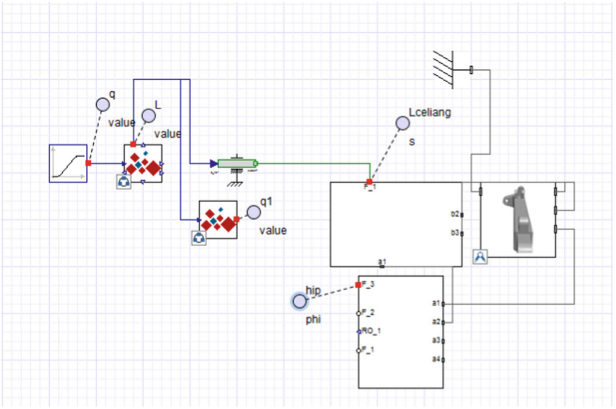

Fig. 3. Model of the hip joint in Maplesim.

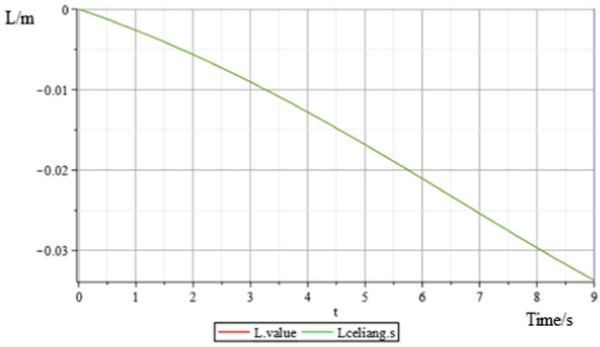

Fig. 4. Simulation results of cylinder expansion.

A hip joint model was established in the simulation software Maplesim, as shown in Fig. 3. q is the input signal of hip joint angle, L is the calculated result of cylinder expansion, Lceliang is the measured result of cylinder expansion, q1 is the hip joint angle obtained by reverse calculation based on cylinder expansion L, and hip is the measured result of hip joint expansion. The simulation results are shown in Fig. 4.

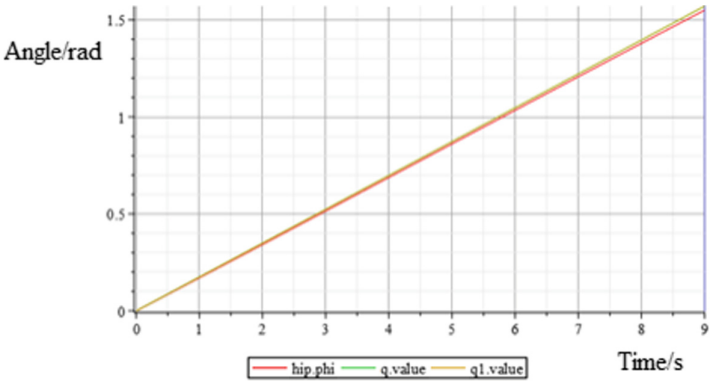

Fig. 5. Simulation results of hip joint angle.

It can be seen from the figure that the calculation result L of cylinder expansion is coincident with the simulation result Lceliang of cylinder expansion.

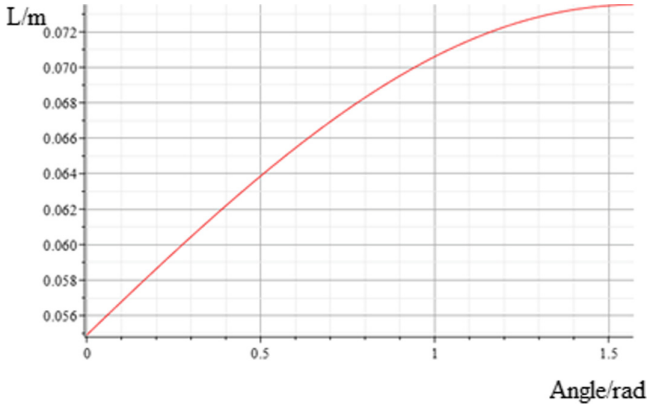

Fig. 6. Relationship between hip joint moment arm and hip joint rotation angle.

As shown in Fig. 5, the input signal q of hip joint angle completely overlaps with the simulation result hip of hip joint angle, and basically overlaps with the hip joint angle q1 obtained by reverse calculation, with a maximum error of 0.02 rad.

The relationship between hip joint moment arm and hip joint angle is shown in Fig. 6.

As can be seen from the figure, with the increase of hip joint angle, the thrust arm also increases, and there is a positive correlation between them.

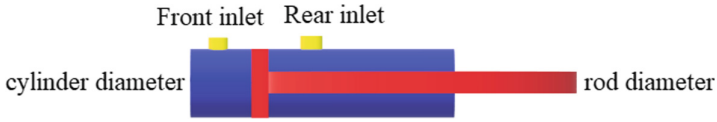

Fig. 7. Schematic diagram of hip cylinder.

Figure 7 shows a schematic diagram of the hip cylinder. The forward inlet extends the cylinder forward and the backward inlet retracts the cylinder backward. Assume that the forward inlet pressure measured by the sensor is P_1, the backward inlet pressure is P_2, the cylinder diameter is D_1, the rod diameter is D_2, the forward thrust of the cylinder is positive, and the backward thrust is negative, then the cylinder thrust expression is.

$$\mathrm{F} = \mathrm{P}_1 * \frac{\mathrm{D}_1^2 * \pi}{4} - \mathrm{P}_2 * \frac{\left(\mathrm{D}_1^2 - \mathrm{D}_2^2\right) * \pi}{4}. \tag{5}$$

Thus, the expression of hip joint torque can be expressed as

$$T = F * \mathrm{lm}(t) \tag{6}$$

3 Torque Control of the Hip Joint

Incremental PID control algorithm is a control algorithm through the increment of the control quantity (the difference between the control quantity and the last control quantity) for PID control [6]. The system deviation is mainly proportional, integral, differential three operations and linear combination into the control quantity [7], in order to reduce the system error, improve the system response speednd response effect [8].

The hydraulic underlying control of this system adopts the valve control mode. When the servo valve voltage is 5 V (theoretical value), the pressure of two channels of the servo valve is balanced, and the hydraulic cylinder does not move. When the servo valve voltage is greater than 5 V, the pressure in channel 1 of the servo valve is greater than the pressure in channel 2, and the hydraulic cylinder extends outward. When the servo valve voltage is less than 5V, the servo valve 2 channel pressure is greater than 1 channel pressure, at this time, the hydraulic cylinder inward contraction. A hydraulic cylinder drives the hip joint to rotate through a four-link mechanism, thus making it complete the corresponding movement. By establishing the relationship between servo valve control voltage and joint torque, hip joint torque control is accomplished (Fig. 8).

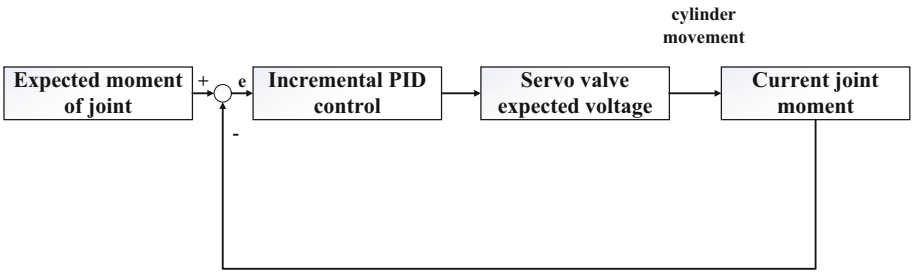

Fig. 8. Block diagram of incremental variable PID torque control of hip joint.

Assume that the joint torque information of the last 3 times fed back by the hip joint is respectively

$$\text{FbkT}[0],\ \text{FbkT}[1],\ \text{FbkT}[2]$$

The expected torque of the hip joint for nearly 3 times is

$$\text{TgtT}[0],\ \text{TgtT}[1],\ \text{TgtT}[2]$$

Let the errors be.

$$\text{Error} = \text{TgtT}[0] - \text{FbkT}[0] \tag{7}$$

$$\text{Error\_pre} = \text{TgtT}[1] - \text{FbkT}[1] \tag{8}$$

$$\text{Error\_last} = \text{TgtT}[2] - \text{FbkT}[2] \tag{9}$$

According to the incremental PID control algorithm formula

$$\Delta u[n] = K_p(e[n] - e[n-1]) + K_i e[n] + K_d(e[n] - 2e[n-1] + e[n-2]) \quad (10)$$

The relationship between servo valve control voltage increment and nearly three times of error is obtained by substituting nearly three times of errointo the formula

$$\Delta u = K_p(\text{Error} - \text{Error\_pre}) + K_i * \text{Error} + K_d(\text{Error} - 2\text{Error\_pre} + \text{Error\_last}) \quad (11)$$

The current control voltage of the servo valve is

$$\begin{aligned} \text{Valve\_u} = \text{Valve\_pre} + \Delta u = \text{Valve\_pre} + K_p(\text{Error} - \text{Error\_pre}) \\ + K_i * \text{Error} + K_d(\text{Error} - 2\text{Error\_pre} + \text{Error\_last}) \end{aligned} \quad (12)$$

Where, Valve_pre is the control voltage of the last servo valve.

The angle of motion of the hip joint ranges from −15° to 90°, and the joint angle is divided into the following four intervals: −15° to 0° (interval 1), 0° to 30° (interval 2), 30° to 60° (interval 3), and 60° to 90° (interval 4). When the hip joint feedback angle is in different intervals, if TgtT[0] − TgtT[1] > 0, take a set of K_p, K_i, K_d and parameters to calculate; If TgtT[0] − TgtT[1] < 0, take another set of parameters for calculation, as shown in the table below.

Table 1. Relationship table between Angle interval and PID parameters.

Angle range	Change of expected moment	
	TgtT[0] − TgtT[1] > 0	TgtT[0] − TgtT[1] < 0
Range 1	K_{p1}, K_{i1}, K_{d1}	K_{p2}, K_{i2}, K_{d2}
Range 2	K_{p3}, K_{i3}, K_{d3}	K_{p4}, K_{i4}, K_{d4}
Range 3	K_{p5}, K_{i5}, K_{d5}	K_{p6}, K_{i6}, K_{d6}
Range 4	K_{p7}, K_{i7}, K_{d7}	K_{p8}, K_{i8}, K_{d8}

For the protection of the servo valve, the output voltage is limited. When the hip joint torque control is carried out, the current expected torque is given. The control voltage of the servo valve is calculated by the incremental variable PID algorithm, and the hydraulic cylinder is controlled to complete the corresponding movement so that the hip joint can output the corresponding torque.

4 Experiments and Conclusions

In order to verify the feasibility of hip joint torque control, the experimental results were carried out on a prototype exoskeleton. Among them, the pressure of the hydraulic

system is 9 MPa, the diameter of the oil cylinder is 20 mm, and the diameter of the rod is 12 mm. Given the expected torques of the hip joint are −120 N * m and 140 N * m respectively, when the expected torques are 140 N * m, the oil cylinder will contract backward to drive the hip joint motion and the torque variation of the hip joint output is shown in Fig. 9.

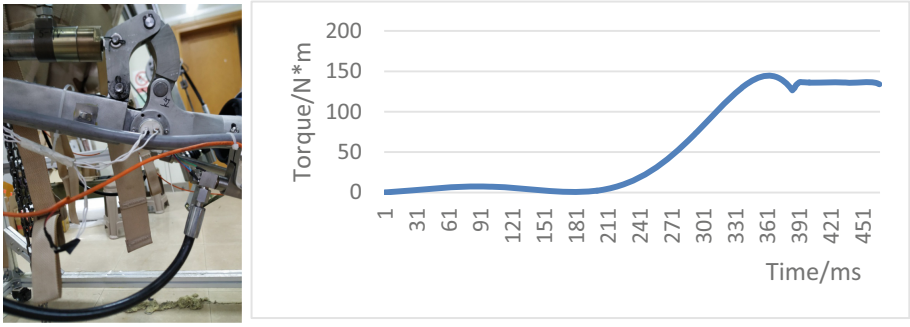

Fig. 9. Hip joint motion and torque diagram (90°).

When the expected torque is −120 N * m, the cylinder is extended forward to drive the hip joint movement and the torque variation of the hip joint output is shown in Fig. 10.

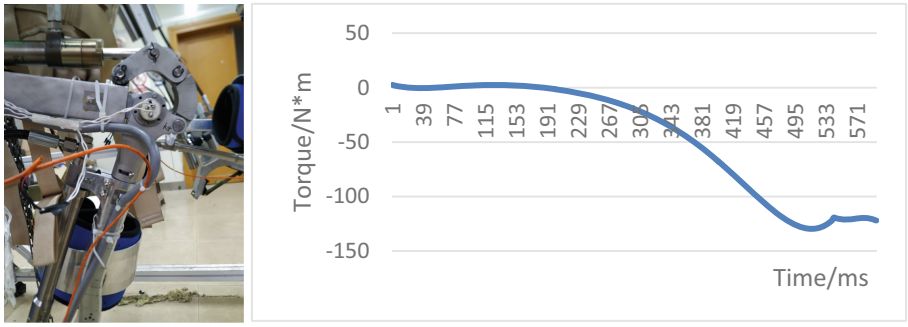

Fig. 10. Hip motion and torque diagram (−15°).

As shown in Fig. 9 and Fig. 10, although there is a certain deviation between the expected torque of hip joint and the feedback torque. We can draw the conclusion from the Table 2 that the average error rate is 2.57% and 1.5% respectively. It can meet the demand of hip joint torque control as a whole. Thus, it can be seen that it is feasible to control the torque of the hip joint without a torque sensor by using the calculated joint torque as feedback.

Table 2. Expected torque versus average calculated torque.

Expected torque (N * m)	Average calculated torque	Average error rate
	(N * m)	(%)
140	136.4	2.57
−120	−121.8	1.5

To sum up, the proposed joint drive system not only achieves lightweight structure, but also achieves high precision torque control without joint torque sensor.

References

1. Jian, W.U.: Research on Joint Drive and Control Technology of Lower Limb Exoskeleton. University of Electronic Science and Technology of China, Chengdu (2019)
2. Young, S.H., Mazzuchi, T.A., Sarkani, S.A.: Frame-work for predicting future system performance in autonomous unmanned ground vehicles. IEEE Trans. Syst. Man Cybern. Syst. **47**(7), 1192–1206 (2017)
3. Endo, Y., Balloch, J.C., Grushin, A., et al.: Landmark-based robust navigation for tactical UGV control in GPS-denied communication-degraded environments. In: SPIE Defense Security. International Society for Optics and Photonics, vol. 98, no. (3), pp. 558–571 (2016)
4. Weijie, J.I.A.: Research on key technologies of BigDog quadruped robot. Inf. Commun. **1**, 25–26 (2018)
5. Wiedehach, C., Bertrand, S., Wu, T., et al.: Walking on partial footholds including line contacts with the humanoid robot atlas. In: IEEE-RAS, International Conference on Humanoid Robots, pp. 1312–1319. IEEE (2017)
6. Wen, Z.: Russian Uran-9 unmanned ground combat vehicle. Ordnance Mater. Sci. Eng. **40**(1), 114 (2017)
7. Yang, L., Zhao, Y., Liu, C.: Development of Russian ground unmanned vehicle. Foreign Tank (10), 110–113 (2017)
8. Wang, J.-L.: Israel shows new ability of unmanned vehicle. Foreign Tank (11), 5 (2016)